The J integral fracture toughness and damage zone morphology in polyethylenes

H. Swei, B. Crist* and S. H. Carr
Departments of Chemical Engineering, and Materials Science & Engineering, Northwestern University, Evanston, IL 60208, USA
(Received 26 March 1990; accepted 21 May 1990)

The J integral analysis of compact tension samples has been used to evaluate plane strain fracture toughness of various polyethylenes at room temperature. Crack propagation commences from a razor notch in high-density polyethylene at $J_{Ic} = 1.7$ kJ m^{-2}. Plastic deformation is confined to a small craze region (about 300 μm long, 20 μm high) through which the crack subsequently propagates. A tough copolymer of PE3408 material resists crack advance until $J_{Ic} = 8.2$ kJ m^{-2}. Here again crack propagation is through a craze, though craze length exceeds 1 mm. Toughness is also imparted by the formation of shear bands near the notch tip. Low-density polyethylene does not really fracture under the present test conditions; this material responds by general yielding and blunting of the notch tip.

(Keywords: fracture toughness; morphology; polyethylenes)

INTRODUCTION

Most semicrystalline and some glassy polymers display considerable ductility at room temperature; when deformed in tension, yielded sections may elongate as much as 10 times before fracturing. If these materials are tested under plane strain conditions, macroscopically 'brittle' failure frequently occurs without large-scale yielding. The study of plane strain fracture in thermoplastics has been motivated by the need to understand and control crack growth in certain applications such as gas distribution pipe[1]. Indeed, one of the first studies of plane strain failure in polyethylene was on a pipe material[2].

Flueler *et al.*[2] and Chan and Williams[3] independently determined the critical stress intensity factor K_{Ic} from three-point bend tests on precracked bars. Sample size requirements for plane strain toughness were similar to those for metals; for high-density polyethylene, $K_{Ic} = 1.0$–1.5 MN m$^{-3/2}$ at room temperature, indicating a bend bar of thickness $B > 10$ mm and of width $W \geqslant 20$ mm[2,3]. It was found that some types of polyethylene were considerably tougher and required testing at subambient temperatures to suppress the yield zone size to that consistent with linear elastic fracture mechanics (LEFM). K_{Ic} was independent of temperature between -120 and -20°C, with material-dependent values[3,4] between 2 and 6 MN m$^{-2/3}$. Measured toughness at low temperature was unchanged by a four-decade variation in deformation rate[4]. Despite the satisfactory use of LEFM and the lack of temperature and rate effects, the plane strain fracture surfaces in polyethylene are not brittle. They show considerable microductility with a characteristic 'tufted' appearance from locally drawn and ruptured fibres; the size scale of these features is typically 10 to 100 μm[2,4].

The need to evaluate fracture behaviour in more ductile and fracture-resistant polyethylenes led to employment by Williams and coworkers[5,6] of the J integral. The primary advantage of this non-linear elastic approach is that the small-scale yielding restriction of LEFM is relaxed, and hence smaller samples suffice to provide a geometry-independent toughness parameter that is characteristic of the material. Another feature of J integral testing is that crack advance Δa must be measured in order to extrapolate J to a critical initiation value J_{Ic} corresponding to $\Delta a \approx 0$. Using procedures established for testing ductile metals[7], special grades of tough high-density polyethylene[5] and linear low-density polyethylene[6] were found to have J_{Ic} in the range 10–40 kJ m^{-2}, increasing with temperature above -80°C. For reference, conventional high-density polyethylene[3] has $K_{Ic} = 1.3$ MN m$^{-3/2}$, which corresponds to $J_{Ic} \approx 1$ kJ m^{-2}. Low-density polyethylene was also tested at temperatures below -20°C, giving $J_{Ic} = 0.5$–2 kJ m^{-2}. Thus J integral testing differentiates between conventional high-density and low-density polyethylenes, both of which have $J_{Ic} \approx 1$ kJ m^{-2}, as opposed to linear low-density polyethylene and selected high-density polyethylenes, which have $J_{Ic} > 10$ kJ m^{-2}. These toughness figures are measured near -20°C, where valid J_{Ic} can be obtained for all materials. The fracture resistance of linear low-density polyethylene has been attributed to toughening by dispersed rubbery particles[8].

Additional J integral testing of polyethylenes at room temperature has been done by Narisawa[9,10]. Rimnac *et al.*[11] considered three-point bend samples of ultrahigh-molecular-weight polyethylene (UHMWPE), for which they report $J_{Ic} = 100$ kJ m^{-2} at room temperature. The plane strain fracture surface of this UHMWPE has none of the tufted appearance seen with other types of polyethylene. Barry and Delatycki[12] have examined the effect of deformation rate on J_{Ic} in a series of high-density polyethylenes at room temperature. Toughness values were in the range 0.2 to 20 kJ m^{-2} and increased by a factor of about 7 with a 10^6 increase in strain rate. A similar rate effect was reported by Jones and Bradley,

* To whom correspondence should be addressed

0032-3861/91/081440-07

who evaluated compact tension specimens obtained from high-density polyethylene pipe[13]. These authors also investigated the effects of precracking techniques, crack propagation direction and annealing on J_{Ic}.

In this work we consider and compare J integral toughness of three different polyethylenes: a high-density polyethylene (HDPE), a conventional low-density polyethylene (LDPE) and a gas pipe (PE3408) based on a copolymer of ethylene and but-1-ene or hex-1-ene[14]. Room-temperature fracture behaviour is quite different for each. Equally significant is the observation that the damage zone through which the crack advances is characteristic for each type of polyethylene. There is a correlation between fracture toughness and the size of the damage zone, which simultaneously supports the relative values of J_{Ic} and provides insight into the origin of toughness in various polyethylenes.

J INTEGRAL TESTING

A procedure for measuring J_{Ic} is described fully in ASTM E813[7]. This is reviewed as background for the methods employed in this study of polymers. The analysis is based on work done in deforming a deeply cracked bend specimen. We use compact tension (CT), samples, for which one writes[7]:

$$J = \frac{U}{B(W-a_0)}\eta \tag{1}$$

Figure 1 is a sketch of the CT geometry; sample width W and precrack length a_0 are measured from the loading line, B is the thickness and H is the distance between loading points. In equation (1) U is the area under the load–displacement curve, and η is a factor that corrects for normal stresses in the uncracked ligament of length $b = (W - a_0)$[7,15]. It is recommended that $H \approx 0.7W$ and $a_0/W = 0.5$–0.7 to ensure that bending dominates the deformation with point loading sufficiently remote from the crack tip. It is also recommended that $0.25 \leqslant B/W \leqslant 0.5$.

The multiple specimen technique is normally used with polymers to establish the relation between J and crack advance Δa. The J values are extrapolated to $\Delta a = 0$ (or some equivalent criterion) to establish J_{Ic}, the critical value of J for the onset of stable crack growth. Data used for extrapolation and hence the determination of J_{Ic} are

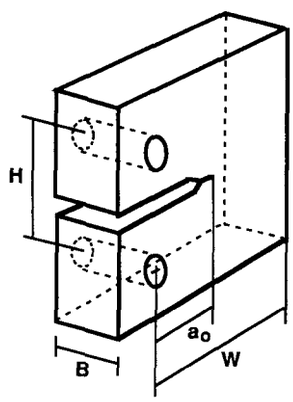

Figure 1 Sketch of compact tension (CT) sample geometry. In this work $B = 12.5$ mm, $W = 23.1$ mm, $a_0 = 11.6$ mm, $H = 15.2$ mm

Table 1 Polymer characterization

Sample	M_w	M_w/M_n	ρ (g cm^{-3})	σ_y (MPa)
HDPE	164 000	11	0.964	26.3
PE3408	–	–	0.949	19.2
LDPE	80 100	4.4	0.919	8.3

subject to the following conditions[7,15]:

$$B > 25J_{Ic}/\sigma_y \tag{2a}$$

$$b > 25J_{Ic}/\sigma_y \tag{2b}$$

$$B > 15J/\sigma_y \tag{3a}$$

$$b > 15J/\sigma_y \tag{3b}$$

$$\Delta a \leqslant 0.06b \tag{4a}$$

$$\omega = (b/J)\,\mathrm{d}J/\mathrm{d}(\Delta a) > 10 \tag{4b}$$

$$\mathrm{d}J/\mathrm{d}(\Delta a) < \sigma_y \tag{4c}$$

Here σ_y is the tensile yield stress or some equivalent measure of flow stress in the ductile material[7].

Equations (2a) and (3a) are to ensure that plane strain conditions are met with a sample of adequate thickness B to suppress through-thickness plastic deformation. Equations (2b) and (3b) express that the uncracked ligament should be large enough to prevent plastic collapse and also to contain the region of the Hutchinson–Rice–Rosengren (HRR) singular field near the crack tip in strain-hardening elastic–plastic materials. Equations (4a) and (4b) are to restrict the amount of physical crack growth and associated unloading for $J > J_{Ic}$; these ensure that initial crack growth is controlled by J. Finally, equation (4c) states that crack growth observed to establish J_{Ic} must be distinguishable from that due to crack-tip blunting.

Extrapolation of J *versus* Δa data, subject to equations (3) and (4) above, is used to establish J_{Ic}. It is customary to extrapolate to a 'blunting line' given by:

$$J_b = 2\sigma_y \Delta a \tag{5}$$

which assumes that the precrack first blunts by shear yielding, and true crack propagation initiates from the blunted crack at $J = J_{Ic}$.

EXPERIMENTAL

Three types of polyethylene were used in these studies: high-density polyethylene (HDPE), PE3408 pipe resin and low-density polyethylene (LDPE). Both HDPE and LDPE were received as 25.4 mm sheet stock from Cadillac Plastics (Chicago, IL). The PE3408 is carbon-filled material from a 330 mm outer diameter, 25.4 mm wall thickness gas distribution pipe generously supplied by Plexco Corporation, Franklin Park, IL. The characteristics of the polymers are shown in *Table 1*. Molecular weights were determined by size exclusion chromatography[16]. Standards for the PE3408 material establish that the melt flow index be less than 0.4[17]. Densities were measured at 23°C in a gradient column; that for PE3408 has been corrected for the presence of 2 wt% carbon[17]. Tensile yield stress was measured at a strain rate of 0.03 min^{-1}, which is the nominal strain rate used in J integral testing.

Compact tension (CT) specimens were prepared as sketched in *Figure 1*. The sides were planar with no side

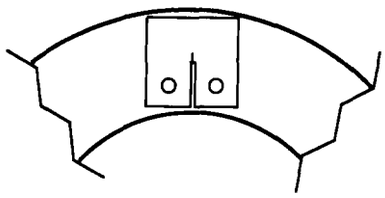

Figure 2 Sketch of PE3408 CT sample in relation to pipe wall

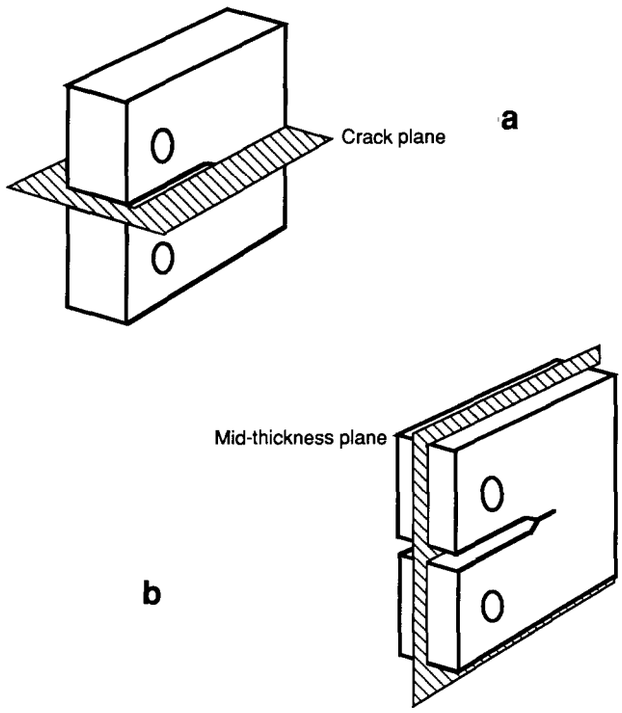

Figure 3 Planes exposed by (a) freeze fracture and (b) transverse sectioning of CT samples

grooves. HDPE and LDPE samples were cut from sheet stock, which was symmetrically milled to leave thickness $B = 12.5$ mm. When samples were cut from HDPE sheet with the crack propagating in the extrusion direction or perpendicular to the extrusion direction, no anisotropy was observed in these tests. PE3408 samples were cut from the gas pipe wall as indicated in *Figure 2*. Crack propagation here corresponds to advance from the inner surface to the outer surface of the wall, with the crack front parallel to the longitudinal axis of the pipe. This conforms to the orientation of 'slit failures' observed in accelerated burst tests[18] and occasional field failures[19]. Note, however, that the inner 50% of the wall thickness in the CT samples is removed by notching and precracking. Precracking was done at room temperature with a fresh razor blade at a cutting rate of 10 mm min^{-1} to achieve $a_0/W = 0.50$. Samples were not tested before one day after razor notching to permit recovery of some of the deformation that accompanies this cutting.

The multiple-specimen regression curve method was used to obtain J as a function of stable crack growth Δa at room temperature. For each polymer, a series of CT samples was loaded to different predetermined levels in an Instron 1125 at a crosshead speed of 0.5 mm min^{-1} (effective strain rate of 0.03 min^{-1}); unloading was at 50 mm min^{-1}. Then J was calculated by equation (1), where U is the area under the load–extension curve up to the point of unloading. Hence J is the sum of both elastic and plastic contributions. The quantity η is 2.26 for the samples used here.

Crack advance Δa was measured after unloading by optical microscopy and scanning electron microscopy (JEOL 100B SEM). Large crack advances were observed on freeze-fractured surfaces (*Figure 3a*), while small crack advances were generally measured from transverse views at the mid-thickness of the CT specimens (*Figure 3b*). Freeze fracture was done by chilling the tested CT sample in liquid nitrogen, then cracking in two with a chisel blow in the machined portion of the precrack. In most cases the region of stable crack growth at room temperature is distinguishable from the surface created by rapid freeze fracture. The transverse plane was exposed by cutting the sample in half as sketched in *Figure 3b*. This surface could be viewed directly by SEM with or without a wedge to open up the crack. Alternatively, a 5 μm section was cut from the mid-thickness region for study by optical microscopy. Final cuts were made at $-121°C$ with a RMC MT6000 ultramicrotome, thereby minimizing distortions of the morphology of interest. SEM samples were coated with 150 Å of gold. Polarized optical microscopy of thin sections was used to evaluate regions of plastic deformation; birefringence gives information on the size of plastic deformation zones and on the average chain orientation within such zones.

RESULTS AND DISCUSSION

High-density polyethylene

As with all the polyethylenes studied in this work, a combination of fracture surface (*Figures 4a* and *4b*) and transverse plane (*Figure 5*) observations was required to define the amount of stable crack advance Δa associated with a particular amount of deformation of the CT sample. Referring to *Figure 4a*, the area of the initial razor notch of length a_0 is labelled as region 1. The area of slow crack growth (region 2) appears as a finely mottled grey field with maximum extension Δa indicated on the figure. Within this area are microfibrillar tufts and dimples having a characteristic dimension of about 10 μm (*Figure 4b*). This crack growth region terminates in a band of appreciably larger fibrils (region 3); these coarse fibrils were present in the unfractured craze ahead of the crack. The craze region appears to end after about 0.3 mm in a transition zone leading to the classic river-bed pattern (region 4) characteristic of brittle fracture. Region 4 results from freeze fracture, being seen in never-loaded samples.

The important distinction between the area of crack advance (region 2) and unbroken craze (region 3) is amplified by the transverse view in *Figure 5*. Here the crack in the half-sample has been wedged open for viewing by SEM. One sees unbroken fibrils of 25 μm diameter clearly demarking the boundary between crack and craze; the craze is about 0.4 mm long, and the crack length in this sample is 0.8 mm.

A graph of J *versus* Δa for HDPE is given in *Figure 6*. Throughout this work Δa is the maximum crack extension at the specimen midplane. While there is some scatter in the data, particularly for $\Delta a > 0.5$ mm, it is certain that no crack advance is seen for $J \leqslant 1.7$ kJ m^{-2}. The data for non-zero Δa values extrapolate to the ordinate to give $J_{Ic} = 1.7$ kJ m^{-2}. A number of points lie to the left of the blunting line, from which it is apparent

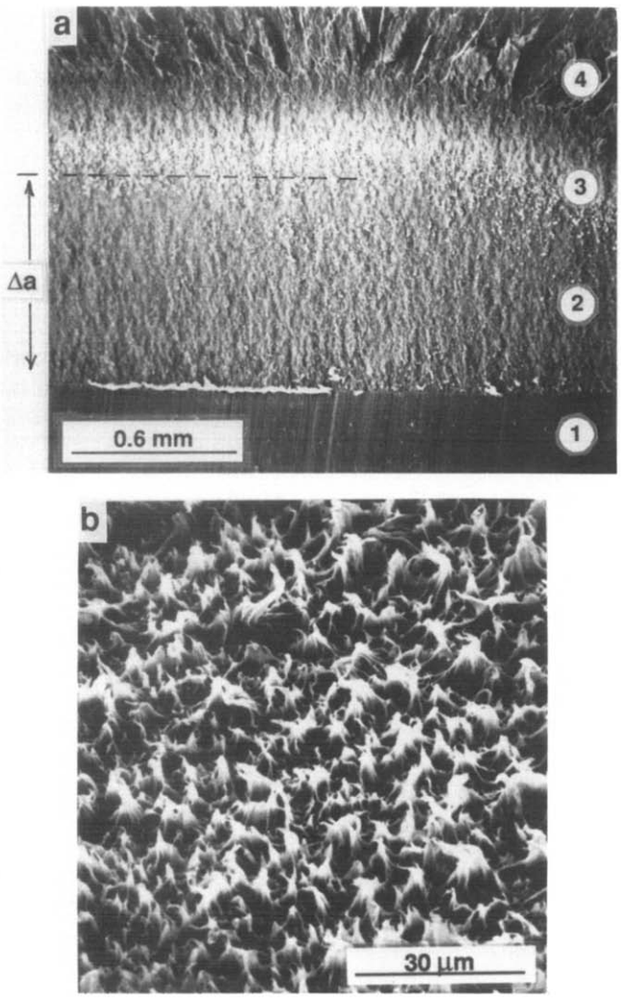

Figure 4 HDPE CT sample. (a) Freeze fracture surface after $J = 1.9$ kJ m^{-2}. See text for explanation of numbered areas. (b) Magnified view of crack growth region 2 in (a)

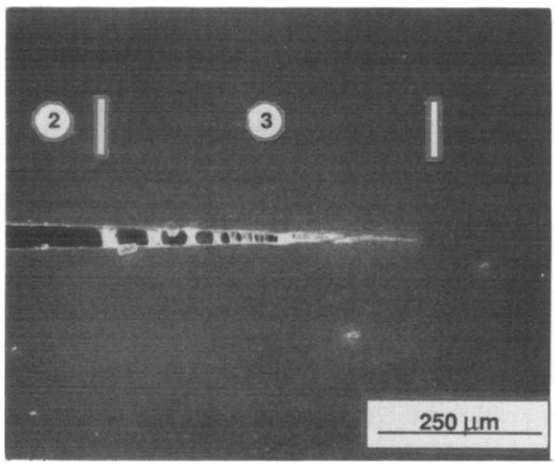

Figure 5 Transverse section of HDPE CT sample after $J = 2.0$ kJ m^{-2}. Numbers correspond to *Figure 4a*

that the crack tip in HDPE does not blunt and advance by yielding as prescribed by equation (5). This is shown further by the sharpness of the crack tip in *Figure 5* (it would have a radius of 0.3 mm according to equation (5)). Finally, optical microscopy of thin sections shows no continuous yielding near the crack tip; birefringence is observed only for the fibrils within crazes or broken fibrils where the crack has advanced. In this we agree with Narisawa and Takemori[20], who found the blunting line inappropriate for determining the initiation of plane strain fracture in toughened polymers.

The various criteria for J integral testing are satisfied by these results. Equation (2) implies that sample thickness B and ligament width b should be greater than 1.6 mm, which are certainly met in the present case. For $B = b = 12.5$ mm, equation (3) allows valid J values as large as 22 kJ m^{-2}, well beyond the observed range. That thickness B is adequate to impose plane strain conditions at the centre is shown by the flatness of the crack front (area 2) in the centre of *Figure 4a*. Similarly, crack growth $\Delta a \leqslant 0.1b$ and $\omega = 4.0$ (equation (4b)). Equation (4c), which is based on the blunting line equation (5), is not applicable to this system.

In earlier work on the same HDPE, Wolf[21] showed that J *versus* Δa plots were fairly insensitive to thickness for $B \geqslant 6.4$ mm, but that larger J values and different behaviour were observed for $B = 3.2$ mm. This manifestation of plane stress contributions in the thinnest sample is consistent with equations (2a) and (3a). It was also observed that the slope of J *versus* Δa plots was very small for $\Delta a > 1.5$ mm ($\Delta a > 0.12b$). Excessive unloading from large crack growth caused equation (4b) to give $\omega < 1$ under these conditions. Extrapolation of such data to $\Delta a = 0$ overestimated J_{Ic} by as much as 50%.

PE3408 pipe material

Crack surface and transverse views are shown in *Figure 7*, and the J *versus* Δa data are in *Figure 8*. The numbered regions in *Figure 7a* are similar to those in *Figure 4a*; the river-bed region 4 begins at the very top of the micrograph. Two major differences from HDPE are apparent: texture within the slow crack growth region 2 is much coarser (characteristic dimension of about 100 μm as opposed to 10 μm), and the size of the region 3 is much larger (1.3 mm *versus* 0.3 mm). Interpretation of these features is again confirmed by transverse sections as in *Figure 7b*. Here one sees in the reflected light optical micrograph a number of long, roughly planar entities;

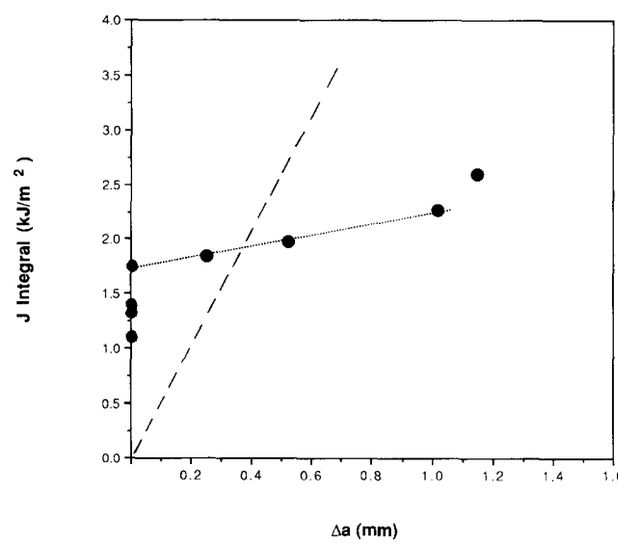

Figure 6 Plot of J integral *versus* crack advance Δa for HDPE. Toughness $J_{Ic} = 1.7$ kJ m^{-2}; blunting line is given by broken line

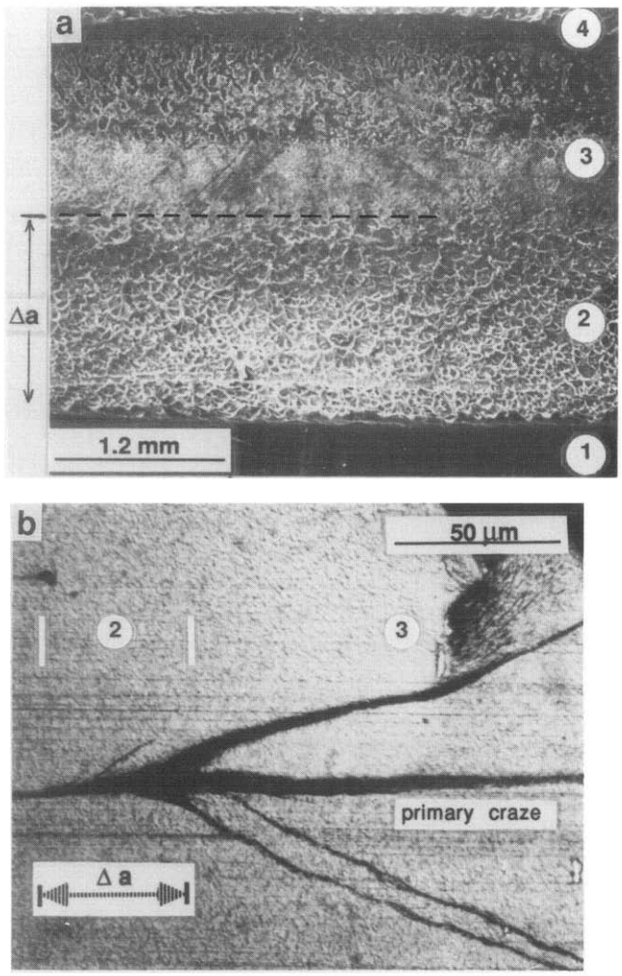

Figure 7 PE3408 CT samples. (a) Freeze fracture surface after $J = 13.4\ \text{kJ m}^{-2}$. See text for explanation of numbered areas. (b) Transverse section after $J = 7.3\ \text{kJ m}^{-2}$

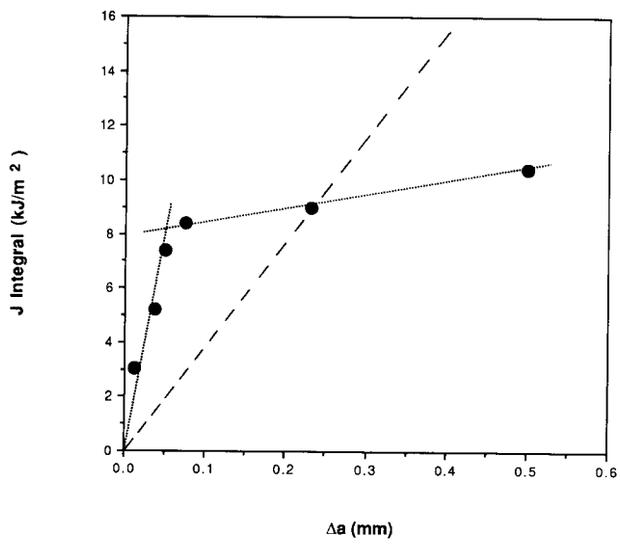

Figure 8 Plot of J integral *versus* crack advance Δa for PE3408. Toughness $J_{Ic} = 8.2\ \text{kJ m}^{-2}$; blunting line is given by broken line

the small crack extension $\Delta a = 0.05$ mm cannot be seen directly in this photograph. The fairly straight feature in the crack plane is indeed a craze of height about 10 μm and length of over 1 mm. The 'flanking' features resemble shear bands as opposed to crazes. This was confirmed by the inclined orientation of these bands with respect to the local tensile stress field and by chain orientation within the bands deduced from birefringence. Crack propagation in PE3408 is by breaking coarse fibrils in the craze. Subsequent freeze fracture rapidly extends the crack through unbroken fibrils in the craze, giving rise to region 3, which has a finer texture than region 2. Region 3 is not observed on the freeze fracture surface of never-loaded CT samples.

The J *versus* Δa data in *Figure 8* appear well behaved. The smallest Δa values are from transverse sections while the larger values are from crack surfaces exposed by freeze fracture. Again, the blunting line does not describe the behaviour before significant crack growth. This is confirmed by the absence of birefringence in the neighbourhood of the crack except within the craze and shear bands. A small amount of crack advance does occur by a type of blunting, however, in which plastic strain in the crack-tip region is localized in craze and shear bands. The J *versus* Δa data show an abrupt change in slope at $J_{Ic} = 8.2\ \text{kJ m}^{-2}$, the point at which crack advance proceeds by fibril breakdown in the craze. Note that *Figure 7b* corresponds to the subcritical or 'blunting' regime; work done on the precracked CT sample goes into forming the large craze and multiple shear bands before real crack growth commences at $J_{Ic} = 8.2\ \text{kJ m}^{-2}$.

Equations (2a) and (2b) require dimensions greater than 10.6 mm for this tougher polyethylene with $J_{Ic} = 8.2\ \text{kJ m}^{-2}$; B and b of 12.5 mm satisfy this condition. Sample thickness B is also seen to be adequate from the flatness of the crack front in *Figure 7a*. Ligament size b is large enough by equation (3b) for $J \leqslant 16\ \text{kJ m}^{-2}$, a ceiling above all the data in *Figure 8*. The generation of a craze longer than 1 mm in a ligament of $b = 12.5$ mm may exacerbate unloading problems, but it should be remembered that a craze supports tensile stress parallel to the craze–matrix interface. The quantity ω equals 6.9 for PE3408, indicating adequate J dominance.

Low-density polyethylene

Freeze fracture and transverse micrographs are in *Figure 9*. The 'crack advance' region 2 in *Figure 9a* appears quite different from those of HDPE (*Figure 4a*) or PE3408 (*Figure 7a*). Region 4 again is the river-bed pattern for low-temperature fracture; there is no region 3. The transverse view in *Figure 9b* shows that yielding and blunting have occurred, followed by some collapse when the CT sample was unloaded. This mechanism of 'crack advance' by yielding and crack-tip blunting is supported by the J *versus* Δa data in *Figure 10*. All the points lie very near to the blunting line, with no indication of crack advance by a true fracture mechanism. Similar behaviour was reported by Hashemi and Williams for linear low-density polyethylenes tested at room temperature[6]. Those polymers have densities, and presumably tensile properties, similar to those of the LDPE used here.

While there is no J_{Ic}, the existence of plane strain is evidenced by the flatness of the 'crack' front in *Figure 9a*. Equations (3a) and (3b) indicate that valid J values as large as $75\ \text{kJ m}^{-2}$ are obtainable with $B = b = 12.5$ mm.

The yield zone was mapped by optical birefringence for a transverse section cut from a CT sample after loading to $J = 4.8\ \text{kJ m}^{-2}$. The zone is sketched in *Figure 11* and has a characteristic size of about 0.2 mm. This is a factor of 2–5 smaller than the plastic zone sizes

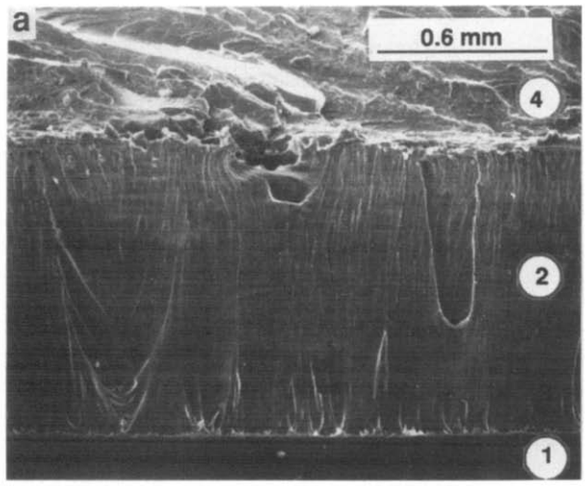

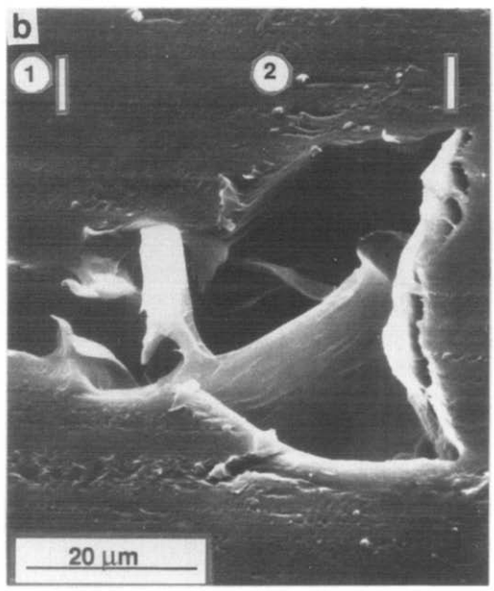

Figure 9 LDPE CT samples. (a) Freeze fracture surface after $J = 16\ \text{kJ m}^{-2}$. See text for explanation of numbered areas. (b) Transverse section after $J = 2.8\ \text{kJ m}^{-2}$

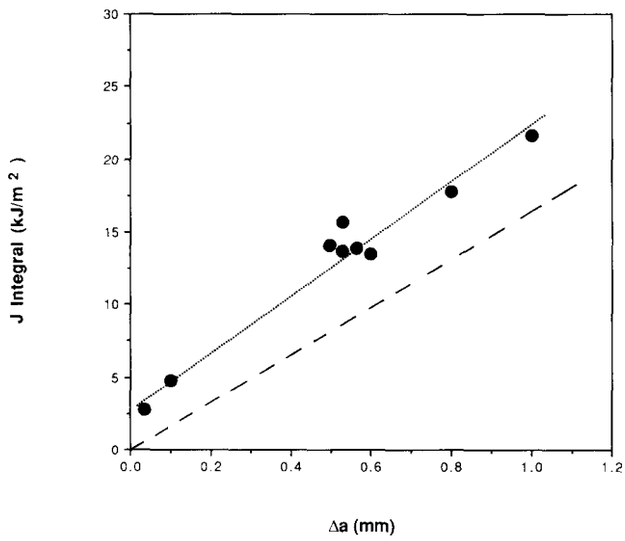

Figure 10 Plot of J integral *versus* crack advance Δa for LDPE. There is no J_{Ic}; blunting line is given by broken line

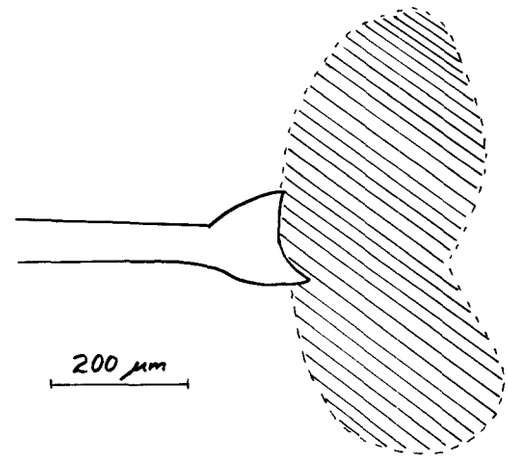

Figure 11 Sketch of crack tip and plastic zone (crosshatched area) in LDPE after $J = 4.8\ \text{kJ m}^{-2}$

calculated using linear elastic–ideal plastic models[22]; the discrepancy undoubtedly arises from the fact that LDPE displays considerable strain hardening[23,24]. It is encouraging, however, to observe that the plastic zone size is moderate with respect to sample dimensions, particularly the ligament size b.

Crack initiation

Some comments about the similarities and differences for crack initiation in HDPE and PE3408 are in order. LDPE is not discussed here because it fractures in a manner of little interest to us. *Figure 12* shows the situation for HDPE at a subcritical value $J < J_{Ic}$. Beyond the razor notch in the region of large triaxial stress are formed numerous voids or microcracks of 1–2 μm extent. These later coalesce to form the craze ahead of the razor notch. The crack propagates through this craze (and the craze propagates ahead of the crack) for $J \geqslant J_{Ic}$; see for example *Figure 5*.

The situation is in many ways similar for the much tougher PE3408 material. Again a craze forms in the plane of the razor notch at a subcritical J; see *Figure 7b*. The major distinction from HDPE is that the craze fibrils are much stronger. Increased loads do not fracture the fibrils before the craze grows to millimetre dimensions and flanking shear bands have formed. How the crack advances through this craze is shown in *Figure 13* for PE3408; $J = 8.4\ \text{kJ m}^{-2}$, which is nearly equal to J_{Ic}. Here, the crack has been wedged open and is about to advance 0.1 mm by failure of the ligament marked 'L'. One also sees the interligament spacing of about 100 μm, accounting for the size scale of the texture in *Figure 7a*. Notice that the flanking yield zones, quite apparent by optical microscopy, are nearly invisible in SEM.

CONCLUSIONS

J integral studies detect significant differences in plane strain fracture of various polyethylenes at room temperature. No crack advance beyond that associated with conventional shear yielding at the crack tip is observed for LDPE. HDPE displays microductile crack growth at $J_{Ic} = 1.7\ \text{kJ m}^{-2}$. Crack advance is through a single craze about 20 μm thick and 0.3 mm long (*Figure 5*). PE3408, an ethylene copolymer used in gas distribution pipes, is

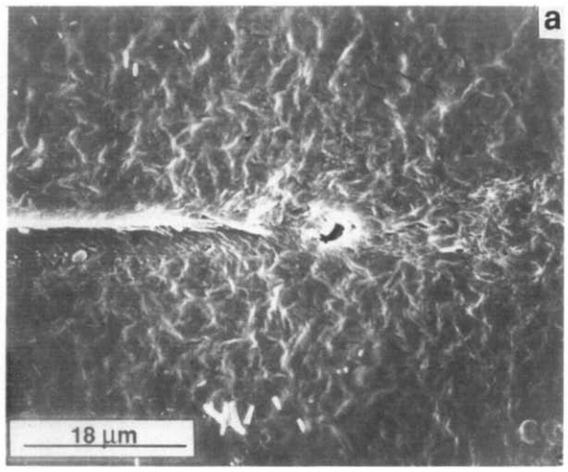

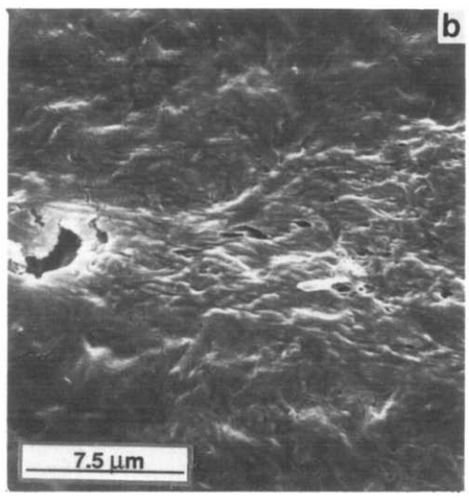

Figure 12 (a) Crack-tip region for HDPE, $J = 1.5$ kJ m^{-2}, for which there is no crack advance. Microcracks about 1 μm long are seen in the higher magnification view (b)

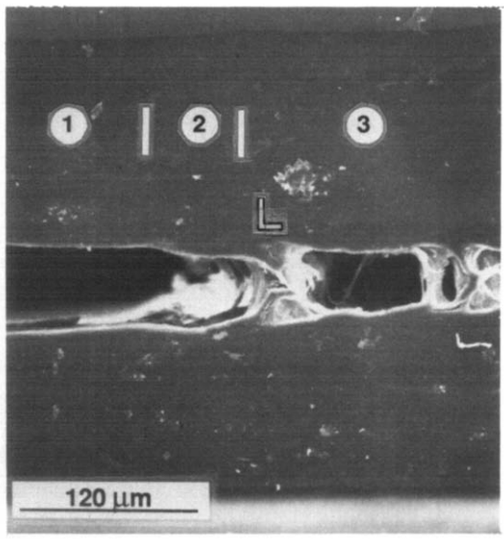

Figure 13 Crack-tip region for PE3408, $J = 8.4$ kJ m^{-2}. Virtually no crack advance has occurred. Numbered regions correspond to those in *Figure 7*

remarkably tougher, with $J_{Ic} = 8.2$ kJ m^{-2}. Enhanced toughness is due to the formation of multiple local plastic zones (craze and shear bands), seen here to be about 10 μm high and 1 mm long, ahead of the crack tip (*Figure 7b*). In neither HDPE nor PE3408 does blunting of the crack tip occur by continuous shear yielding. Plastic deformation is localized to craze regions and, in the case of PE3408, shear bands.

Because of the complex combinations of yielding, crazing and crack advance that occur in plane strain deformation, careful microscopic examination of the crack tip and damage region is required to establish the relevant fracture processes in polyethylene. The most reliable results are obtained by increasing J from very small values and observing where crack growth starts. Extrapolation of large Δa data to determine J_{Ic} may be suspect because of questionable J dominance. Employing the blunting line to determine J_{Ic} is certainly inappropriate for polyethylene and a number of other polymers[20]. The problem is not so much that the derived value of J_{Ic} is affected, but that the mechanisms of plane strain damage and crack initiation are misrepresented.

ACKNOWLEDGEMENTS

This research was supported by the Gas Research Institute, Basic Science Division (Contract No. 5084-260-1051). We thank Professor B. Moran for helpful discussions and Dr L. Wild for the molecular-weight determinations.

REFERENCES

1 Proc. Eleventh Plastic Fuel Gas Pipe Symp., American Gas Association, Arlington, VA, 1989
2 Flueler, P., Roberts, D. R., Mandell, J. F. and McGerry, F. J. in ASTM Special Technical Publication No. 736, American Society for Testing Materials, 1981, p. 15
3 Chan, M. K. V. and Williams, J. G. *Polym. Eng. Sci.* 1981, **21**, 1019
4 Mandell, J. F., Roberts, D. R. and McGerry, F. J. *Polym. Eng. Sci.* 1983, **23**, 404
5 Chan, M. K. V. and Williams, J. G. *Int. J. Fracture* 1983, **23**, 145
6 Hashemi, S. and Williams, J. G. *Polymer* 1986, **27**, 384
7 ASTM E813, in 'Annual Book of ASTM Standards', American Society for Testing Materials, 1987, Vol. 03.01
8 Mirabella, F. M., Westphal, S. P., Fernando, P. L., Ford, E. A. and Williams, J. G. *J. Polym. Sci. (B) Polym. Phys.* 1988, **26**, 1995
9 Narisawa, I. and Nishimura, H. in Proc. Tenth Plastic Fuel Gas Pipe Symp., American Gas Association, Arlington, VA, 1987, pp. 268–277
10 Narisawa, I. *Polym. Eng. Sci.* 1987, **27**, 41
11 Rimnac, C. M., Wright, T. M. and Klein, R. W. *Polym. Eng. Sci.* 1988, **28**, 1586
12 Barry, D. B. and Delatycki, O. *J. Appl. Polym. Sci.* 1989, **38**, 339
13 Jones, R. E. and Bradley, W. L. in ASTM Special Technical Publication No. 995, American Society for Testing Materials, 1989, p. 447
14 Leech, J. R. in Proc. Ninth Plastic Fuel Gas Pipe Symp., American Gas Association, Arlington, VA, 1985, pp. 3–16
15 Kanninen, M. F. and Popelar, C. H. 'Advanced Fracture Mechanics', Oxford University Press, New York, 1985, Ch. 5
16 Wild, L. Quantum Chemicals/USI, private communication
17 ASTM D3350, in 'Annual Book of ASTM Standards', American Society for Testing Materials, 1987, Vol. 08.03
18 Henrich, R. C. in Proc. Eighth Plastic Fuel Gas Pipe Symp., American Gas Association, Arlington, VA, 1983, pp. 84–95
19 Lustinger, A. in ref. 18, pp. 176–179
20 Narisawa, I. and Takemori, M. *Polym. Eng. Sci.* 1989, **29**, 671
21 Wolf, A. L. MS Thesis, Northwestern University, 1986
22 Williams, J. G. *Adv. Polym. Sci.* 1978, **27**, 67
23 Metaxas, C. PhD Thesis, Northwestern University, 1991
24 Mills, P. J., Hay, J. N. and Hayward, R. N. *J. Mater. Sci.* 1985, **20**, 501